Supplementary: Statistical Inference Models for Image Datasets with Systematic Variations

Won Hwa Kim[†¶] Barbara B. Bendlin[*¶] Moo K. Chung[§] Sterling C. Johnson[*¶] Vikas Singh[§†¶]

[†]Dept. of Computer Sciences, University of Wisconsin, Madison, WI
[§]Dept. of Biostatistics & Med. Informatics, University of Wisconsin, Madison, WI
[¶]Wisconsin Alzheimer's Disease Research Center, University of Wisconsin, Madison, WI
[*]GRECC, William S. Middleton VA Hospital, Madison, WI

1. Proof of Proposition 3.

Proposition 3. Let λ^I, λ^J and χ^I and χ^J denote the eigenvalues and eigenvectors from graphs of I and J respectively. Then, the WKD $d_s(p^I, q^J)$ can be written as,

$$d_s(p^I,q^J)^2 = \sum_{l_1=0}^{N-1} g(s\lambda^I_{l_1})^2 \chi^I_{l_1}(p)^2 + \sum_{l_2=0}^{N-1} g(s\lambda^J_{l_2})^2 \chi^J_{l_2}(q)^2 - 2\sum_{l_1,l_2=0}^{N-1} g(s\lambda^I_{l_1})\chi^I_{l_1}(p) g(s\lambda^J_{l_2})\chi^J_{l_2}(q)\langle \chi^I_{l_1}, \chi^J_{l_2}\rangle \tag{1}$$

Proof. Let X be a square integrable space and $\{\lambda^I_l, \chi^I_l\}$ and $\{\lambda^J_l, \chi^J_l\}$ be eigenvalue and eigenvector pairs from graph Laplacians of graph I and J respectively.

$$\begin{aligned}
d_s(p^I,q^J)^2 &= ||\psi^I_s(p,r) - \psi^J_s(q,r)||^2_2 \\
&= \int_X (\psi^I_s(p,r) - \psi^J_s(q,r))^2 d\mu(r) \\
&= \int_X \psi^I_s(p,r)^2 + \psi^J_s(p,r)^2 - 2\psi^I_s(p,r)\psi^J_s(q,r) d\mu(r) \\
&= \int_X (\sum_{l_1=0}^{N-1} g(s\lambda^I_{l_1})\chi^I_{l_1}(p)\chi^I_{l_1}(r))^2 + (\sum_{l_2=0}^{N-1} g(s\lambda^J_{l_2})\chi^J_{l_2}(q)\chi^J_{l_2}(r))^2 \\
&\quad - 2\sum_{l_1,l_2=0}^{N-1} g(s\lambda^I_{l_1})\chi^I_{l_1}(p)\chi^I_{l_1}(r) g(s\lambda^J_{l_2})\chi^J_{l_2}(q)\chi^J_{l_2}(r)\, d\mu(r) \\
&= \sum_{l_1=0}^{N-1} g(s\lambda^I_{l_1})^2\chi^I_{l_1}(p)^2 \int_X \chi^I_{l_1}(r)^2 d\mu(r) + \sum_{l_2=0}^{N-1} g(s\lambda^J_{l_2})^2\chi^J_{l_2}(q)^2 \int_X \chi^J_{l_2}(r)^2 d\mu(r) \\
&\quad - 2\sum_{l_1,l_2=0}^{N-1} g(s\lambda^I_{l_1})\chi^I_{l_1}(p) g(s\lambda^J_{l_2})\chi^J_{l_2}(q) \int_X \chi^I_{l_1}(r)\chi^J_n(r)\, d\mu(r) \\
&= \sum_{l_1=0}^{N-1} g(s\lambda^I_{l_1})^2 \chi^I_{l_1}(p)^2 + \sum_{l_2=0}^{N-1} g(s\lambda^J_{l_2})^2 \chi^J_{l_2}(q)^2 - 2\sum_{l_1,l_2=0}^{N-1} g(s\lambda^I_{l_1})\chi^I_{l_1}(p) g(s\lambda^J_{l_2})\chi^J_{l_2}(q)\langle \chi^I_{l_1}, \chi^J_{l_2}\rangle
\end{aligned}$$

□

2. Correlation with a Gray matter Mask

Note that when performing hypothesis testing at the voxel level, one needs to perform a multiple comparisons correction to control for Type 1 errors. This correction typically depends on the number of hypothesis tests being performed. Therefore, if we are repeating the test over the entire brain image, the p-values coming out of the statistical tests need to be very small to survive this correction. Typically, due to physiological processes that the images capture, with knowledge of the imaging modality, it is reasonable to remove some regions of the image where the specific modality is unlikely to reveal pathologies or group differences. For instance, in PIB-PET images, we may focus our analysis only in the gray matter region and ignore white matter regions. Using standard software tools, a segmentation of the brain into white matter, gray matter and cerebrospinal fluid (CSF) can easily provide 'masks' — our analysis can then focus only on the regions within the mask. We show these results below in Fig. 1.

After masking, the number of voxels that survive threshold at correlation level 0.3 is reduced to 18060 (3.54%) from $21101(4.13\%)$ using WKD, but it still outperforms the 14010 voxels (2.74%) identified to be statistically significant using the original SUVR images.

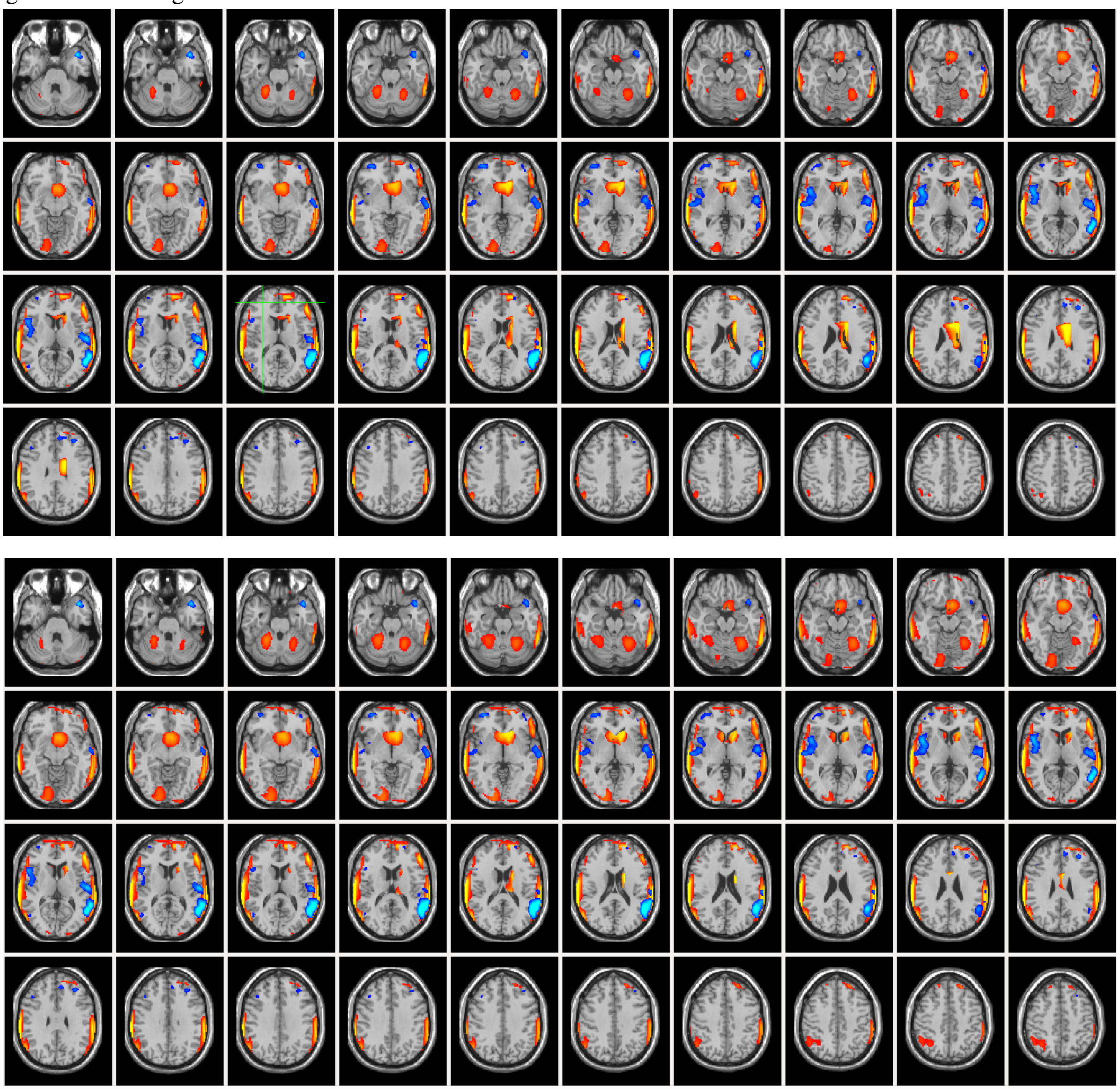

Figure 1. Montage of axial view of the correlation between the PIB changes and the ratio of total τ-protein and Aβ(1-42) on a template T1-weighted brain image. The red-yellow intensities indicate correlation using WKD, and the blue-light blue intensities indicates correlation using SUVR images in the range of $[0.3\ 0.5]$. Top: Correlation before gray-matter masking, Bottom: Correlation after masking with a gray-matter mask.

3. More results on NASA Images

In this supplementary, we exhibit more experiment results of change detection from NASA Observatory images (`http://earthobservatory.nasa.gov`). The experiments are carried in the same manner as in the original paper, where we have two images from two time points where there is a subtle difference due to temperature change, flooding, fire and so on. The latter image is flipped by dividing the image by -1. Now, assuming that we do not know the normalization parameter, the images cannot be compared directly. In Fig. 2

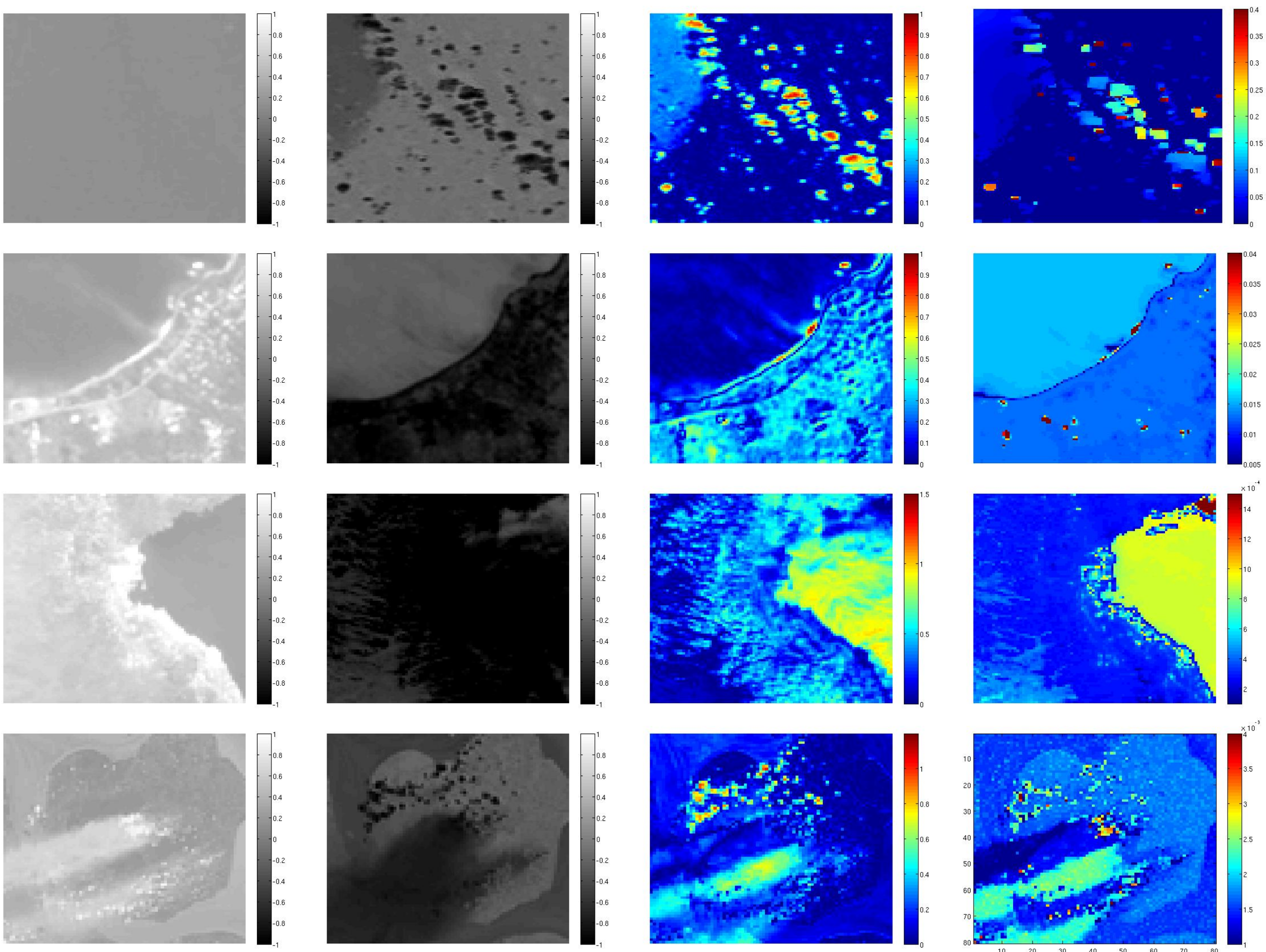

Figure 2. More results from NASA Earth Observatory images. We detect the changes between two images (in different scales) of various satellite images from all over the world. First column: images taken in 2013, Second column: images taken in 2014 (flipped), Third column: ground truth, Fourth column: changes identified using WKD.

4. More results on NASA Images

Implementation of the framework in Matlab (for 2D images) is provided in the supplementary. Example images from the NASA Observatory images (on Sierra Nevada, CA) are also included along with the implementation.